

# Three-dimensional effects in “atom diodes”: atom-optical devices for one-way motion

A. Ruschhaupt\*

*Institut für Mathematische Physik, TU Braunschweig,  
Mendelssohnstrasse 3, 38106 Braunschweig, Germany*

J. G. Muga†

*Departamento de Química-Física, Universidad del País Vasco, Apdo. 644, 48080 Bilbao, Spain*

The “atom diode” is a laser device that lets the ground state atom pass in one direction but not in the opposite direction. We examine three-dimensional effects of that device for arbitrary atomic incidence angles on flat laser sheets and set breakdown limiting angles and velocities. It is found that a correct diodic behavior independent of the incident angle can be obtained with blue detuned lasers.

PACS numbers: 03.75.Be,42.50.Lc

## I. INTRODUCTION

Atom optics is “basically the development and perfection of techniques and devices which can manipulate the atom waves coherently” [1]. Many of these devices (lenses, mirrors, beam splitters) have their origin in standard light optics, and others are influenced by electronics: this has led to the idea of guiding the atoms in atomic circuits and developing circuit control elements. We have proposed in particular, in analogy with the electronic diode, an “atom diode” [2, 3, 4], a laser device which combines state-selective mirrors and pumping lasers to let the neutral atom in its ground state pass in one direction (conventionally from left to right), but not in the opposite direction for a range of incident velocities. Similar ideas have been put forward independently by Raizen and coworkers [5, 6] who proposed one-way barriers to implement a new laser cooling technique sweeping them across an atomic trap. The near possibility of an experimental implementation has motivated a recent analysis on the effect of quenching lasers to improve the diode performance [4], as well as the present work, which investigates three dimensional (3D) effects that had been ignored so far, and the way to overcome them. The original models have been one-dimensional, which is appropriate for tight lateral confinement in wave guides or cigar shaped traps, but for general geometries, and in particular for flat laser sheets and arbitrary incidence angles, three dimensional effects may become important as we shall see. As a further motivation, consider an interesting application of the atom diode shown schematically in Fig. 1, namely a realization of Maxwell’s pressure demon [7, 8, 9, 10]: Starting with a box of atoms at random positions we put an atom diode in the middle (the direction of transmission is indicated by an arrow). After some time, all atoms will be on the right-hand side of the box provided that the diode works independently of atomic

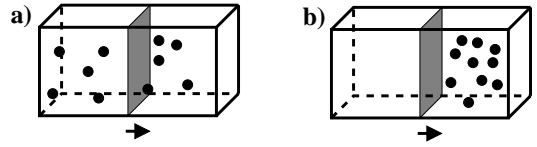


FIG. 1: A version of Maxwell’s demon: the atom diode would achieve a differential of pressure as an inanimate one-way valve, by letting atoms cross in one direction but not in the opposite one.

velocity and incident angle.

The paper begins with an analysis of the 2-level diode in Sec. II, and Sec. III discusses the 3-level diode: this is a worthwhile complication since it provides a simple physical realization of the former case with just two lasers by adiabatic elimination.

Throughout the paper, flat laser sheets are assumed to extend in the  $y - z$ -plane with some thickness in  $x$ -direction, and laser wave-vectors point in  $y$ -direction. Because of translational symmetry in  $z$ -direction and the corresponding conservation of  $z$ -momentum, this coordinate will be ignored hereafter.

## II. ATOM DIODE BASED ON 2 LEVELS PLUS QUENCHING

The basic setting for a two-level atom diode can be seen in Fig. 2a and 2c, and consists of three, partially overlapping, interaction regions: in the external ones, state-selective mirrors block the excited ( $|2\rangle$ ) and ground ( $|1\rangle$ ) state atoms, respectively; in the central pumping region, a laser, possibly detuned with respect to the atomic transition with detuning  $\Delta_P$  (the difference between the pumping laser frequency and atomic transition frequency  $\omega_{21}$  between levels 1 and 2) couples the two levels. The pumping laser has a wave vector of modulus  $k_P > 0$  in  $y$  direction and the Rabi frequency is  $\Omega_P$ . The detuning, which is a novel feature with respect to our previous work, plays an important role in 3D as we shall see. In

\*Email address: a.ruschhaupt@tu-bs.de

†Email address: jg.muga@ehu.es

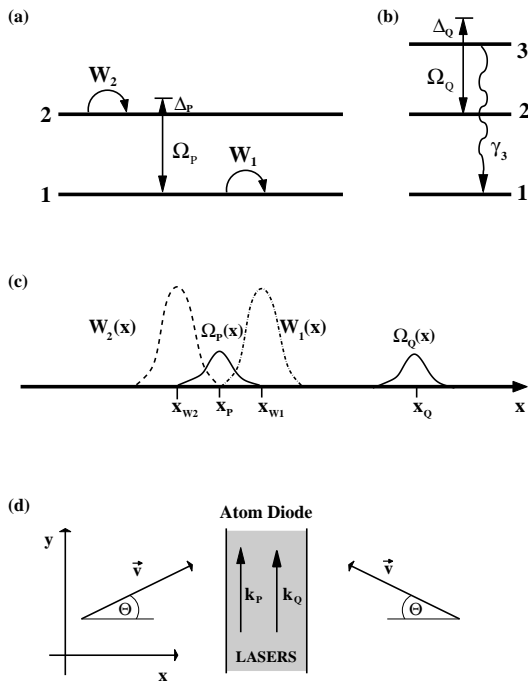


FIG. 2: Atom diode based on 2 levels plus quenching: (a,b) Schematic action of the different lasers on the atom levels, (c) location of the different laser potentials in  $x$  direction, and (d) setting in the  $x - y$  plane.

principle it is possible to implement this scheme with three different lasers, one for each region, nevertheless a simpler realization relies on just two lasers appropriately detuned and a STIRAP (Stimulated Raman Adiabatic Passage [11]) process, this case is worked out in Sec. III as a generalization of the results discussed in [3].

The explanation of the diodic behavior is the following (see Fig. 2c): If the ground-state atom travels from the right to left and its velocity is not too high, it is reflected by the state-selective mirror potential  $W_1\hbar/2$  and returns to the right. If the atom travels from the left in the ground state, it will cross the potential  $W_2\hbar/2$ , be pumped to the second level and pass to the right unaffected by the potential  $W_1\hbar/2$ . It might seem that  $W_2\hbar/2$  plays no role but, if it is removed, the transmittance  $1 \rightarrow 2$  from the left drops dramatically [3]. The role and importance of the state-selective mirror potentials is thus not reduced to blocking. Their presence is essential to facilitate an adiabatic rightwards transfer of population from state 1 to state 2 [3]. This makes the device quite robust and insensitive to shape or parameter variations, in particular reflection and transmission probabilities become in 1D flat functions of the velocity for broad intervals. In 3D, these intervals will in general also depend on the incidence angle, but later we shall show that this dependence can be suppressed using an appropriate detuning.

For many applications, the atom should decay irreversibly back to the ground state after crossing the three

regions to avoid any backwards motion from right to left. The decay can occur naturally or be forced by an additional quenching laser pumping the atom to a third state which decays to the ground state with a fast rate  $\gamma_3$ , see Fig. 2b. The quenching laser interaction is characterized by a wave vector of modulus  $k_Q > 0$  in  $y$  direction, Rabi frequency  $\Omega_Q$ , and detuning  $\Delta_Q$  (difference between the laser frequency and the transition frequency  $\omega_{32}$ ).

The atom dynamics corresponding to Fig. 2 can be described by a master equation or equivalently by the quantum jump formalism [13]. However, to determine the working conditions of the diode, it is enough to examine the evolution until the first spontaneous decay of the atom, since, with the chosen laser configuration, it is extremely unlikely that there will be more than one spontaneous decay. This evolution is described by an effective Schrödinger-equation dynamics in the quantum jump approach. Using the rotating-wave approximation, and in a laser adapted interaction picture such that the Hamiltonian is time independent, the corresponding effective Hamiltonian is

$$H_2 = \frac{p_x^2}{2m} + \frac{p_y^2}{2m} + \frac{\hbar}{2} \begin{pmatrix} W_1(x) & \Omega_P(x)e^{-ik_P y} & 0 \\ \Omega_P(x)e^{ik_P y} & W_2(x) - 2\Delta_P & \Omega_Q(x)e^{-ik_Q y} \\ 0 & \Omega_Q(x)e^{ik_Q y} & -i\gamma_3 - 2(\Delta_Q + \Delta_P) \end{pmatrix},$$

with  $|1\rangle \equiv \begin{pmatrix} 1 \\ 0 \\ 0 \end{pmatrix}$ ,  $|2\rangle \equiv \begin{pmatrix} 0 \\ 1 \\ 0 \end{pmatrix}$ , and  $|3\rangle \equiv \begin{pmatrix} 0 \\ 0 \\ 1 \end{pmatrix}$ .  $p_x = -i\hbar\frac{\partial}{\partial x}$  and  $p_y = -i\hbar\frac{\partial}{\partial y}$  are the momentum operator components in  $x - y$  space, and  $m$  is the mass (corresponding to Neon in all numerical examples).  $W_1(x)\hbar/2$  and  $W_2(x)\hbar/2$  are the effective reflecting potentials. Their dependence on  $x$  only (and not on  $y$ ) is justified in the Appendix for a three-laser realization of the 2-level diode, and in section III for a two-laser realization. We have  $k_P = k_{P0} + \frac{\Delta_P}{c}$  and  $k_Q = k_{Q0} + \frac{\Delta_Q}{c}$  with  $k_{P0} = \frac{\omega_{21}}{c}$  and  $k_{Q0} = \frac{\omega_{32}}{c}$  (we assume  $\omega_3 > \omega_2 > \omega_1$ ).

We will examine the stationary Schrödinger equation

$$E\Psi(x, y) = H_2\Psi(x, y) \quad (1)$$

with  $E = \frac{\hbar^2}{2m}(k_x^2 + k_y^2)$ ,  $k_x := \frac{m}{\hbar}v \cos \Theta \geq 0$ ,  $k_y := \frac{m}{\hbar}v \sin \Theta$ , and  $v = |\vec{v}|$  (see Fig. 2d). To disentangle different effects we shall first analyze the diode part shown in Fig. 2a and determine the optimal working conditions for which atoms coming from the right are reflected and atoms from the left are transmitted. Then we shall study the quenching laser alone, as in Fig. 2b, and finally combine everything.

### A. Effective one-dimensional equations

The two-dimensional equation (1) can be transformed into an effective one-dimensional one by inserting the

ansatz

$$\Psi(x, y) = \begin{pmatrix} \phi_1(x)e^{ik_y y} \\ \phi_2(x)e^{i(k_y+k_P)y} \\ \phi_3(x)e^{i(k_y+k_P+k_Q)y} \end{pmatrix}.$$

Then we get

$$\frac{\hbar^2 k_x^2}{2m} \begin{pmatrix} \phi_1(x) \\ \phi_2(x) \\ \phi_3(x) \end{pmatrix} = \left[ \frac{p_x^2}{2m} + \frac{\hbar}{2} \begin{pmatrix} W_1(x) & \Omega_P(x) & 0 \\ \Omega_P(x) & W_2(x) - 2\Delta_{3d,2} & \Omega_Q(x) \\ 0 & \Omega_Q(x) & -2(\Delta_{3d,2} + \Delta_{3d,3}) - i\gamma_3 \end{pmatrix} \right] \begin{pmatrix} \phi_1(x) \\ \phi_2(x) \\ \phi_3(x) \end{pmatrix}, \quad (2)$$

where

$$\begin{aligned} \Delta_{3d,2} &= \Delta_P - \frac{\hbar}{2m}(2k_y k_P + k_P^2) \\ \Delta_{3d,3} &= \Delta_Q - \frac{\hbar}{2m}[2(k_y + k_P)k_Q + k_Q^2] \end{aligned}$$

are effective “three-dimensional” detunings which include Doppler and recoil terms.

### B. Diode without quenching

First we shall study the part of the atom diode shown in Fig. 2a by setting  $\Omega_Q = 0$ ,  $\gamma_3 = 0$ . Let us consider left incidence in the ground state. Then the asymptotic form of  $\Psi$  is

$$\begin{aligned} \Psi(x, y) &\stackrel{x \ll 0}{\approx} \begin{pmatrix} e^{ik_x x + ik_y y} \\ 0 \\ 0 \end{pmatrix} \\ &\quad + \begin{pmatrix} R_{11}e^{-ik_x x + ik_y y} \\ R_{21}e^{-iqx + i(k_y + k_P)y} \\ 0 \end{pmatrix}, \\ \Psi(x, y) &\stackrel{x \gg 0}{\approx} \begin{pmatrix} T_{11}e^{ik_x x + ik_y y} \\ T_{21}e^{iqx + i(k_y + k_P)y} \\ 0 \end{pmatrix}, \end{aligned}$$

with

$$\begin{aligned} q &= \sqrt{k_x^2 - k_P^2 - 2k_y k_P + 2m\Delta_P/\hbar} \\ &= \frac{m}{\hbar} \sqrt{v^2 \cos^2 \Theta - v_P^2 - 2v_P v \sin \Theta + 2c\Delta v_P}, \end{aligned} \quad (3)$$

where  $v_P = v_{P0} + \Delta v_P$ ,  $v_{P0} = \hbar k_{P0}/m$ , and  $\Delta v_P = \hbar\Delta_P/(mc)$ . We denote by  $R_{\beta\alpha} = R_{\beta\alpha}(w > 0, \Theta)$  the reflection amplitudes for incidence with modulus of velocity  $w = v > 0$  and incidence angle  $\Theta$  from the left in channel  $\alpha$ , and reflection in channel  $\beta$ . Similarly we denote by  $T_{\beta\alpha} = T_{\beta\alpha}(w > 0, \Theta)$  the transmission amplitudes for incidence in channel  $\alpha$  from the left and transmission in channel  $\beta$ . The reflection and transmission coefficients can be simply calculated for the effective one-dimensional equation (2) with the effective “three-dimensional” de-

tunings. Perfect “diodic” behavior means full transmission for left incidence, i.e.

$$\frac{\text{Re}(q)}{k_x} |T_{21}|^2 \approx 1, \quad (4)$$

such that the approximate, asymptotic form of  $\Psi$  is

$$\Psi(x, y) \stackrel{x \ll 0}{\approx} \begin{pmatrix} e^{ik_x x + ik_y y} \\ 0 \\ 0 \end{pmatrix}, \quad (5)$$

$$\Psi(x, y) \stackrel{x \gg 0}{\approx} \begin{pmatrix} 0 \\ T_{21}e^{iqx + i(k_y + k_P)y} \\ 0 \end{pmatrix}. \quad (6)$$

The important point is that, for having a traveling (and no evanescent) transmitted wave and for fulfilling Eq. (4),  $q$  must be real. From this condition we can derive a lower boundary for  $k_x$  at an incidence angle  $\Theta$ , namely

$$k_x^2 \geq k_L^2 + 2k_y k_L - 2m\Delta_P/\hbar. \quad (7)$$

Note that atomic incidence opposite to the laser direction is more efficient than incidence in the same direction because of the Doppler effect. In this later case ( $k_y > 0$ ), a positive (blue) detuning may compensate the effect of Doppler and recoil terms. Because the detuning is much smaller than the transition frequency  $\omega_{21}$ ,  $k_P \approx k_{P0}$ . So we can write the condition (7) as

$$v^2 \cos^2 \Theta - 2v_{P0}v \sin \Theta + 2c\Delta v_P - v_{P0}^2 \geq 0. \quad (8)$$

Let us now consider incidence from the right in the ground state. The asymptotic form for the wave function is then

$$\begin{aligned} \Psi(x, y) &\stackrel{x \gg 0}{\approx} \begin{pmatrix} e^{-ik_x x + ik_y y} \\ 0 \\ 0 \end{pmatrix} \\ &\quad + \begin{pmatrix} R_{11}e^{ik_x x + ik_y y} \\ R_{21}e^{iqx + i(k_y + k_P)y} \\ 0 \end{pmatrix}, \\ \Psi(x, y) &\stackrel{x \ll 0}{\approx} \begin{pmatrix} T_{11}e^{-ik_x x + ik_y y} \\ T_{21}e^{-iqx + i(k_y + k_P)y} \\ 0 \end{pmatrix}, \end{aligned}$$

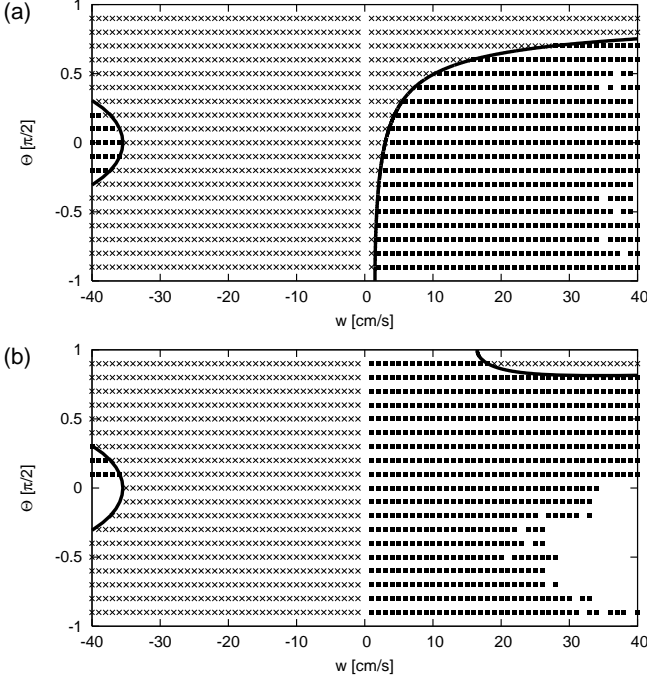


FIG. 3: Dioidic behavior based on 2 levels without quenching: full reflexion (crosses), full transmission (boxes), otherwise (blanks);  $d = 50 \mu\text{m}$ ,  $\sigma = 15 \mu\text{m}$ ,  $\hat{\Omega}_P = 10^6 \text{s}^{-1}$ ,  $\hat{W}_1 = \hat{W}_2 = 4 \times 10^7 \text{s}^{-1}$ ,  $v_{P0} = 3 \text{cm/s}$ ; (a)  $\Delta v_P = 0$ ; (b)  $\Delta v_P = 1.8 \times 10^{-9} \text{cm/s}$ ; the solid line on the left indicates the boundary following from Eq. (9) and the one on the right the boundary resulting from Eq. (8).

where the right incidence will be indicated, if necessary, with a negative argument  $w$  in transmission and reflection amplitudes,  $w = -v < 0$ . Perfect “dioidic” behavior means now full reflection, i.e.  $|R_{11}|^2 \approx 1$ . An approximate condition for this to happen is that  $\frac{\hbar^2}{2m} k_x^2 \leq \frac{\hbar}{2} \hat{W}_1$ , where  $\hat{W}_1 = \max_x W_1(x)$ , and therefore we get a velocity bound for full reflection, namely

$$v \leq \sqrt{\frac{\hbar \hat{W}_1}{m} \frac{1}{\cos \Theta}}. \quad (9)$$

Note that this bound is symmetrical with respect to normal incidence because the mirror barrier height, by hypothesis, does not depend on the incident angle, see the Appendix for the physical justification.

A numerical example can be found in Fig. 3. The shapes of the Rabi frequency and the reflecting potentials are Gaussian,  $\Omega_P(x) = \hat{\Omega}_P \Pi(x, 0)$ ,  $W_1(x) = \hat{W}_1 \Pi(x, d)$ , and  $W_2(x) = \hat{W}_2 \Pi(x, -d)$ , with

$$\Pi(x, x_0) = \exp\left(-\frac{(x - x_0)^2}{2\sigma^2}\right). \quad (10)$$

Full reflexion is indicated with crosses, more precisely

this means

$$(1.0 - |R_{11}|^2) + \frac{\text{Re}(q)}{k_x} |R_{21}|^2 + |T_{11}|^2 + \frac{\text{Re}(q)}{k_x} |T_{21}|^2 < 0.01. \quad (11)$$

Full transmission is indicated by boxes, this means

$$|R_{11}|^2 + \frac{\text{Re}(q)}{k_x} |R_{21}|^2 + |T_{11}|^2 + \left(1.0 - \frac{\text{Re}(q)}{k_x} |T_{21}|^2\right) < 0.01, \quad (12)$$

an any other result is left blank.

Let us first discuss the case of incidence from the right ( $w < 0$ ): We can see in Figs. 3 that the breakdown of the full reflexion is very well approximated by the boundary (9) (left solid line). The diode is fully reflecting the ground state atoms independently of the incident angle and detuning for  $v \lesssim 35 \text{cm/s}$ .

For left incidence,  $w > 0$ , in Fig. 3a with an on-resonance pumping laser, the range of the diodic behavior is not independent of the angle, and there is no  $v_{max}$  such that the atoms incident from the left are transmitted for all velocities  $w \leq v_{max}$  independently of the angle of incidence. The minimal velocity for transmission can be approximated by the boundary (8) (see the right solid line in the figure). As shown in Fig. 3b, full transmission for the lowest velocities can be realized independently of the angle by using detuning  $\Delta_P$ : now the atom diode is working for  $v \leq v_{max} \approx 16 \text{cm/s}$  for left and right incidence independently of the angle of incidence. Increasing the detuning,  $v_{max}$  cannot be increased to arbitrarily high values, because of the earlier breakdown of the adiabatic transmission (see the blanks in Fig. 3b). Nevertheless, the breakdown velocity of the adiabatic transmission can be increased by increasing the laser intensities.

### C. Quenching

We shall now consider the quenching laser alone, as in Fig. 2b, i.e. we set  $\Omega_P = 0$ ,  $W_1 = 0$ , and  $W_2 = 0$ , but  $\Omega_Q > 0$  and  $\gamma_3 > 0$ . Also, we restrict ourselves to the case of incidence from the left. Motivated by the full transmission case of the last subsection, see Eq. (6), we assume that the asymptotic forms are

$$\Psi(x, y) \stackrel{x \ll 0}{\sim} \begin{pmatrix} 0 \\ e^{iqx + i(k_y + k_P)y} \\ 0 \end{pmatrix} + \begin{pmatrix} 0 \\ R_{22} e^{-iqx + i(k_y + k_P)y} \\ R_{32} e^{-iq'x + i(k_y + k_P + k_Q)y} \end{pmatrix},$$

$$\Psi(x, y) \stackrel{x \gg 0}{\sim} \begin{pmatrix} 0 \\ T_{22} e^{iqx + i(k_y + k_P)y} \\ T_{32} e^{iq'x + i(k_y + k_P + k_Q)y} \end{pmatrix},$$

with  $q = q(w, \Theta)$  given by Eq. (4) and  $q' = \sqrt{q^2 - k_Q^2 - 2(k_y + k_P)k_Q + 2m\Delta_Q/\hbar}$ . Note that we have included an incident wavenumber  $k_P$  in  $y$  direction since we assume that the atom has previously passed successfully the diode of Fig. 2a. A spontaneous decay should happen with high probability, therefore the goal is now nearly full absorption, i.e. all reflection and transmission coefficients should vanish. We have examined this numerically in Fig. 4 where  $v_{Q0} = \hbar k_{Q0}/m$  and  $\Delta v_Q = \hbar\Delta_Q/(mc)$ . The triangles mark velocities  $w = v > 0$  and angles  $\Theta$  where we get practically full absorption, i.e.  $|R_{22}|^2 + \frac{\text{Re}(q')}{q} |R_{32}|^2 + |T_{22}|^2 + \frac{\text{Re}(q')}{q} |T_{32}|^2 < 0.01$ . We get practically full absorption independent of the incidence angle  $\Theta$  for  $w \lesssim 16$  cm/s.

Two different reasons for failure may be identified: in the upper part of the figure, the solid line is the bound for evanescent waves in Eq. (8). In the surrounded blank region there is no wave with real momentum incident on the quenching potential, i.e.  $q$  is imaginary. The other blank regions are due to the failure of absorption with  $T_{22} \neq 0$  because of a weak quenching. A simple understanding of the boundary shapes found follows from a complex potential approximation, as in the Appendix, a Schrödinger equation for level 2 of (2) can be written in terms of a complex potential  $W_{eff}\hbar/2$ ,

$$\frac{\hbar^2 k_x^2}{2m} \phi_2(x) = \frac{p_x^2}{2m} \phi_2(x) + \frac{\hbar}{2} [\Omega_P(x)\phi_1(x) + (W_2(x) - 2\Delta_{3d,2} + W_{eff}(x))\phi_2(x)]$$

with

$$W_{eff}(x) = \frac{2\Delta_{3d,3}\Omega_Q(x)^2}{4\Delta_{3d,3}^2 + \gamma_3^2} - i \underbrace{\frac{\gamma_3\Omega_Q(x)^2}{4\Delta_{3d,3}^2 + \gamma_3^2}}_{\gamma_{eff}(x)}.$$

Absorption will fail when the crossing time  $\sim \frac{\sigma}{v_x}$  ( $\sigma$  being the width of the quenching laser, see Eq.(10)) is lower than the corresponding lifetime  $\sim 1/\gamma_{eff}$ , i.e. an approximate condition for absorption is

$$\frac{\gamma\hat{\Omega}_Q^2}{4\Delta_{3d,3}^2 + \gamma_3^2} \cdot \frac{\sigma}{v_x} > \beta$$

with  $\beta$  being a fitting constant. The boundaries following from this condition with  $\beta = 3$  are plotted in Fig. 4 by dashed lines. For negative (see. Fig. 4a)/positive (see. Fig. 4c) detuning,  $\gamma_{eff}$  is maximal at negative/positive angles, respectively, and decreases otherwise. The effect of small absorption, and large lifetime, is however compensated for very oblique incidence, so that the crossing time is even larger than the lifetime: this explains the roughly parabolic profiles of the dashed lines. The absorption failure regions will shrink by increasing laser intensity. The zero detuning case is globally advantageous and we shall restrict to it in the following.

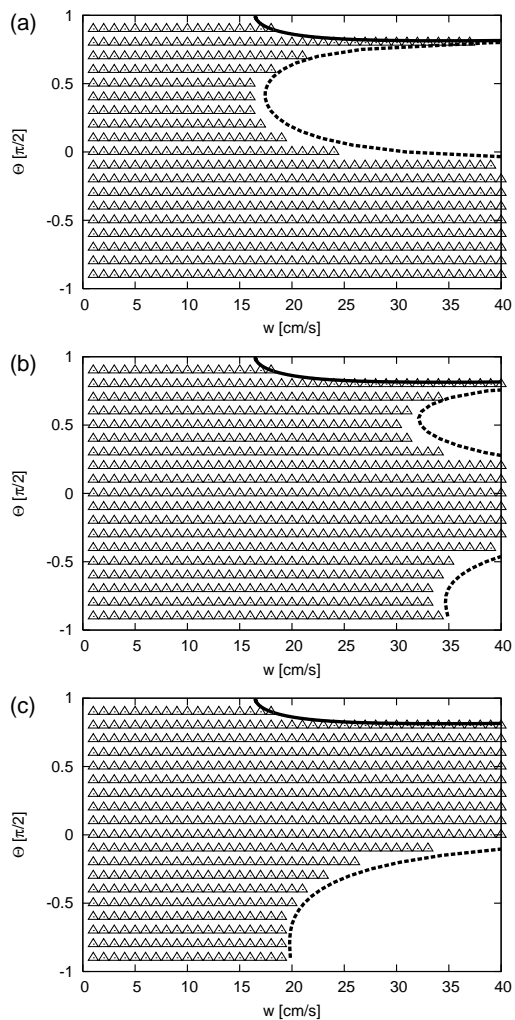


FIG. 4: Quenching: the triangles indicate full absorption;  $\hat{\Omega}_Q = 2 \times 10^6 \text{ s}^{-1}$ ,  $v_{Q0} = 3 \text{ cm/s}$ ,  $\gamma_3 = 3 \times 10^5 \text{ s}^{-1}$ , (a)  $\Delta v_Q = -1.8 \times 10^{-9} \text{ cm/s}$ ; (b)  $\Delta v_Q = 0$ ; (c)  $\Delta v_Q = 1.8 \times 10^{-9} \text{ cm/s}$ ; for other parameters see Fig. 3b.

#### D. Diode with quenching

Now we are ready to combine the diode and the quenching laser as in Fig. 2c and we restrict again the analysis to incidence from the left. We use the parameters of Fig. 3b and Fig. 4b and the result is plotted in Fig. 5: the filled triangles mark velocities and angles for which we get full transmission through the first three regions without quenching laser and full absorption if the quenching laser is switched on, i.e. the atom diode is working: because with the chosen laser configuration, it is extremely likely that the excited atom will decay in the quenching region after it has passed the mirror potential  $W_2\hbar/2$  and therefore it will move finally to the right-hand side. This happens for velocities  $w \lesssim 16 \text{ cm/s}$  independently of the angle of incidence  $\Theta$ . The breakdown at high velocities in Fig. 5 has different reasons:

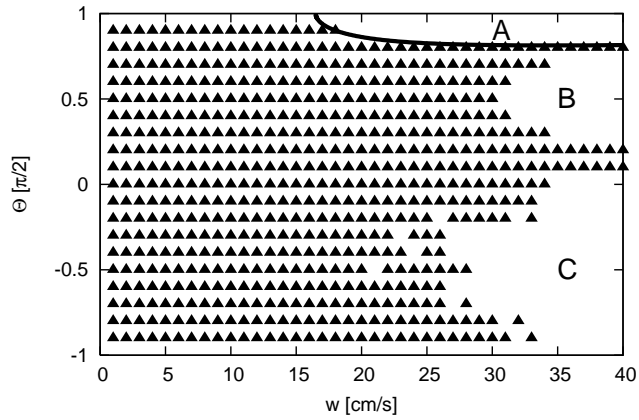


FIG. 5: Dioidic behavior based on 2 levels plus quenching: the filled triangles indicate full transmission to the second state without quenching laser and full absorption if a quenching potential is added; the characters indicate regions of different breakdown reasons as explained in the main text; parameters in Figs. 3b and 4b.

in the blank region A (bordered by the solid line) there is full reflection instead of transmission to state 2; in the blank region B the quenching process fails (compare to Fig. 4b); and in the blank region C the pumping process to state 2 fails, compare to Fig. 3b.

### III. ATOM DIODE BASED ON 3 LEVELS PLUS QUENCHING

An atom diode may also be realized with the three level scheme shown in Figs. 5a and 5c. The basic idea is to combine two lasers that achieve STIRAP (stimulated Raman adiabatic passage) with a state-selective reflecting interaction for the ground state. The STIRAP method is well known [11] and consists of an adiabatic transfer of population between levels 1 and 3 by two partially overlapping (here in space, see Fig. 5c) laser beams coupling 1 and 3 with a further level 2, in a somewhat counterintuitive order. The pump laser couples the atomic levels 1 and 2 with Rabi frequency  $\Omega_P$ , and the Stokes laser couples the states 2 and 3 with Rabi frequency  $\Omega_S$ . Because by a STIRAP transfer the atom is (ideally) transferred from  $1 \rightarrow 3$  without being in 2 the transfer is essentially not affected by a possible decay  $2 \rightarrow 1$ . If we add a third laser causing an effective reflecting potential  $W(x)\hbar/2$  for the ground state component, an atom incident from the

right in the ground state and with low enough velocity is reflected by the potential  $W(x)\hbar/2$  and will finally travel to the right.

If the atom comes from the left in the ground state, it will be transferred by STIRAP to the third state. Therefore the moving atom in the third state is not affected by  $W(x)$ . If quenching is included, see Fig. 5b, it will be pumped to a fourth level by the quenching laser and de-

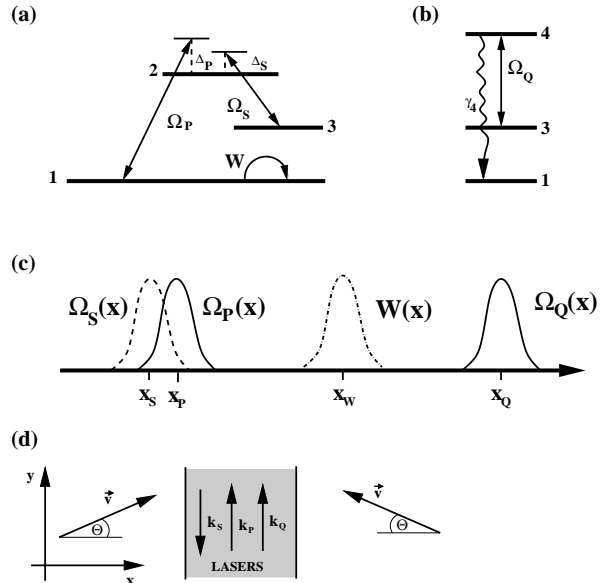


FIG. 6: Atom diode based on 3 levels plus quenching: (a,b) Schematic action of the different lasers on the atom levels, (c) location of the different laser potentials in  $x$  direction, and (d) setting in the  $x-y$  plane.

cay to the ground state. Another possibility is to pump it to the second level again if this level decays fast to the ground state [4]. Finally the atom will travel to the right in the ground state.

Analogously to the previous section, it is sufficient to examine an effective stationary Schrödinger equation which takes now the form

$$E\Psi(x, y) = H_3\Psi(x, y) \quad (13)$$

with  $E = \frac{\hbar^2}{2m}(k_x^2 + k_y^2)$ ,  $k_x := \frac{m}{\hbar}v \cos \Theta \geq 0$ ,  $k_y := \frac{m}{\hbar}v \sin \Theta$ , and  $v = |\vec{v}|$  (see Fig. 6d). The effective Hamiltonian is given by

$$H_3 = \frac{p_x^2}{2m} + \frac{p_y^2}{2m} + \frac{\hbar}{2} \begin{pmatrix} W(x) & \Omega_P(x)e^{-ik_P y} & 0 & 0 \\ \Omega_P(x)e^{ik_P y} & -2\Delta_P & \Omega_S(x)e^{ik_S y} & 0 \\ 0 & \Omega_S(x)e^{-ik_S y} & -2\Delta_P + 2\Delta_S & \Omega_Q(x)e^{-ik_Q y} \\ 0 & 0 & \Omega_Q(x)e^{ik_Q y} & -2\Delta_P + 2\Delta_S - i\gamma_4 \end{pmatrix}.$$

$k_P$  is chosen similarly to the previous section. The Stokes laser has a wave vector of modulus  $k_S > 0$  in  $-y$  direction. We get  $k_S = k_{S0} + \frac{\Delta_S}{c}$  with  $k_{S0} = \frac{\omega_2 - \omega_3}{c}$ . The on-resonance quenching laser has a wave vector in  $y$  direction of modulus  $k_Q = \frac{\omega_4 - \omega_3}{c}$ . Note that we assume for the frequencies of the atomic levels  $\omega_4 > \omega_2 > \omega_3 > \omega_1$ .

### A. Reduction to the 2 level plus quenching case

This level and laser scheme without mirror potential, i.e.  $W(x) = 0$ , can be used to realize the two-level case and potentials of the previous section in the limit of highly detuned lasers. In [3] we have discussed a similar result in the one-dimensional case. We shall show now that this reduction is also valid in three dimensions and including a final detuning in the effective pumping interaction. Let  $\Psi = (\psi_1, \psi_2, \psi_3, \psi_4)^T$ . Equation (13) for

the second component  $\psi_2$  with  $W(x) = 0$  is given by

$$\left[ E - \left( \frac{p_x^2}{2m} + \frac{p_y^2}{2m} \right) + \hbar\Delta_P \right] \psi_2(x, y) = \frac{\hbar}{2} \Omega_P(x) e^{ik_P y} \psi_1(x, y) + \frac{\hbar}{2} \Omega_S(x) e^{iks y} \psi_3(x, y).$$

In the case of large detuning  $\Delta_P$  we may write heuristically

$$\psi_2(x, y) \approx \frac{1}{2\Delta_P} \left[ \Omega_P(x) e^{ik_P y} \psi_1(x, y) + \Omega_S(x) e^{iks y} \psi_3(x, y) \right].$$

We assume that  $\Delta_S$  is also large such that  $\Delta_P - \Delta_S$  is “small”. Putting the approximate expression for  $\psi_2$  in the equations for the other components we get

$$E \begin{pmatrix} \psi_1(x, y) \\ \psi_3(x, y) \\ \psi_4(x, y) \end{pmatrix} = \left[ \frac{p_x^2}{2m} + \frac{p_y^2}{2m} + \frac{\hbar}{2} \begin{pmatrix} \widetilde{W}_1(x) & \widetilde{\Omega}(x) e^{-i\tilde{k}_L y} & 0 \\ \widetilde{\Omega}(x) e^{i\tilde{k}_L y} & \widetilde{W}_3(x) - 2\widetilde{\Delta} & \Omega_Q(x) e^{-ik_Q y} \\ 0 & \Omega_Q(x) e^{ik_Q y} & -2\widetilde{\Delta} - i\gamma_4 \end{pmatrix} \right] \begin{pmatrix} \psi_1(x, y) \\ \psi_3(x, y) \\ \psi_4(x, y) \end{pmatrix}$$

with

$$\widetilde{W}_1(x) = \frac{\Omega_P(x)^2}{2\Delta_P}, \quad \widetilde{W}_3(x) = \frac{\Omega_S(x)^2}{2\Delta_P}, \quad \widetilde{\Omega}(x) = \frac{\Omega_P(x)\Omega_S(x)}{2\Delta_P}, \quad \tilde{k}_L = k_P - k_S, \quad \widetilde{\Delta} = \Delta_P - \Delta_S,$$

which has the same structure as Eq. (1). The two lasers provide state-selective reflecting mirrors in the extremes, and a pumping interaction in their overlapping region with an effective wavenumber and detuning equal to the differences between wavenumbers and detunings.

### B. Effective one-dimensional equation

Now we return to Eq. (13). Again we can rewrite the equation as an effective one-dimensional equation by inserting the ansatz

$$\Psi(x, y) = \begin{pmatrix} \phi_1(x) e^{ik_y y} \\ \phi_2(x) e^{i(k_y + k_P) y} \\ \phi_3(x) e^{i(k_y + k_P - k_S) y} \\ \phi_4(x) e^{i(k_y + k_P - k_S + k_Q) y} \end{pmatrix}$$

to get

$$\frac{\hbar^2 k_x^2}{2m} \begin{pmatrix} \phi_1(x) \\ \phi_2(x) \\ \phi_3(x) \\ \phi_4(x) \end{pmatrix} = \left[ \frac{p_x^2}{2m} + \frac{\hbar}{2} \begin{pmatrix} W(x) & \Omega_P(x) & 0 & 0 \\ \Omega_P(x) & -2\Delta_{3d,2} & \Omega_S(x) & 0 \\ 0 & \Omega_S(x) & -2(\Delta_{3d,2} + \Delta_{3d,3}) & \Omega_Q(x) \\ 0 & 0 & \Omega_Q(x) & -2(\Delta_{3d,2} + \Delta_{3d,3} + \Delta_{3d,4}) - i\gamma_4 \end{pmatrix} \right] \begin{pmatrix} \phi_1(x) \\ \phi_2(x) \\ \phi_3(x) \\ \phi_4(x) \end{pmatrix},$$

where the effective “three-dimensional” detunings are defined by

$$\Delta_{3d,2} = \Delta_P - \frac{\hbar}{2m} (2k_y k_P + k_P^2),$$

$$\Delta_{3d,3} = -\Delta_S - \frac{\hbar}{2m} (-2(k_y + k_P)k_S + k_S^2),$$

$$\Delta_{3d,4} = -\frac{\hbar}{2m} (2(k_y + k_P - k_S)k_Q + k_Q^2).$$

### C. Diodic behavior

Similarly to the previous section we first want to derive some boundary conditions for the diodic behavior. For right incidence, we get the same upper boundary (9) for full reflection. For left incidence in the ground state and without a quenching laser ( $\Omega_Q = 0, \gamma_4 = 0$ ) the asymptotic form is

$$\Psi(x, y) \stackrel{x \ll 0}{\approx} \begin{pmatrix} e^{ik_x x + ik_y y} \\ 0 \\ 0 \\ 0 \end{pmatrix} + \begin{pmatrix} R_{11} e^{-ik_x x + ik_y y} \\ R_{21} e^{-iqx + i(k_y + k_P)y} \\ R_{31} e^{-iq'x + i(k_y + k_P - k_S)y} \\ 0 \end{pmatrix},$$

$$\Psi(x, y) \stackrel{x \gg 0}{\approx} \begin{pmatrix} T_{11} e^{ik_x x + ik_y y} \\ T_{21} e^{iqx + i(k_y + k_P)y} \\ T_{31} e^{iq'x + i(k_y + k_P - k_S)y} \\ 0 \end{pmatrix},$$

with  $k_x = \frac{m}{\hbar} v \cos \Theta \geq 0$ ,  $k_y = \frac{m}{\hbar} v \sin \Theta$ ,  $q = \sqrt{k_x^2 - k_P^2 - 2k_y k_P + 2m\Delta_P/\hbar}$ , and  $q' = \sqrt{k_x^2 - (k_P - k_S)^2 - 2k_y(k_P - k_S) + 2m(\Delta_P - \Delta_S)/\hbar}$ . Following the same arguments as in the previous section, we get a lower boundary for perfect transmission in state 3 (i.e.  $\frac{\text{Re}(q')}{k_x} |T_{31}^l|^2 \approx 1$ ) for left incidence, namely

$$v^2 \cos^2 \Theta - 2v \sin \Theta v_{PS} + \Delta v_{PS} - v_{PS}^2 \geq 0, \quad (14)$$

where  $v_{PS} = \hbar(k_{P0} - k_{S0})/m$  and  $\Delta v_{PS} = \hbar(\Delta_P - \Delta_S)/(mc)$ .

A numerical example without quenching can be found in Fig. 7. The shapes of the Rabi frequency and the reflecting potentials in the model are again Gaussian,  $\Omega_S(x) = \hat{\Omega}_S \Pi(x, x_S)$ ,  $\Omega_P(x) = \hat{\Omega}_P \Pi(x, x_P)$ , and  $W(x) = \hat{W} \Pi(x, x_W)$ . Full reflection (crosses) and full transmission to the third state (boxes) are defined by a straightforward extension of the condition (11) resp. (12). Again, detuning is needed to fulfill the requirement of a diode behavior independent of the angle, see Fig. 7b for  $v \lesssim 17$  cm/s. Detuning causes STIRAP to break down earlier, as in Fig. 3b for the two level model, nevertheless this breakdown can be pushed to higher velocities by increasing laser intensities. The result if the quenching laser ( $\Omega_Q(x) = \hat{\Omega}_Q \Pi(x, x_Q)$ ) is included is shown in Fig. 8 for incidence from the left. The results are very similar to those of the two-level model, the diode including quenching works for velocities  $v \lesssim 17$  cm/s independently of the angle of incidence  $\Theta$ .

### IV. SUMMARY

The prospects to realize in the laboratory atom diodes, i.e. one-way laser barriers, for selective trapping, cooling,

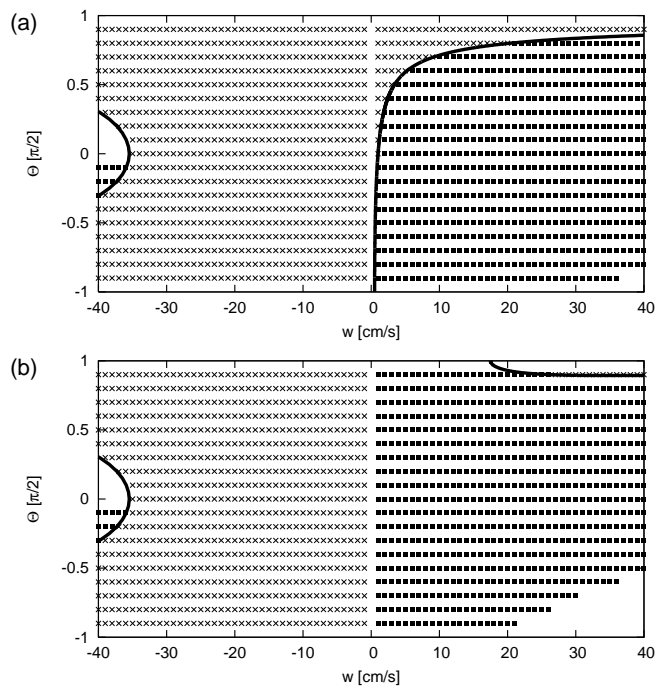


FIG. 7: Diodic behavior based on 3 levels without quenching: full reflexion (crossed), full transmission (boxes), otherwise (blanks);  $\hat{\Omega}_S = \hat{\Omega}_P = 6 \times 10^6 \text{ s}^{-1}$ ,  $\hat{W} = 4 \times 10^7 \text{ s}^{-1}$ ,  $x_S = -20 \mu\text{m}$ ,  $x_P = 20 \mu\text{m}$ ,  $x_W = 85 \mu\text{m}$ ,  $v_{P0} = 3 \text{ cm/s}$ ,  $v_{S0} = 2 \text{ cm/s}$ ,  $\Delta_S = 0$ ; (a)  $\Delta v_{PS} = 0$ ; (b)  $\Delta v_{PS} = 0.6 \times 10^{-9} \text{ cm/s}$ ; the solid line on the left indicates the boundary following from Eq. (9) and the one on the right the boundary resulting from Eq. (14).

implementing a Maxwell pressure demon, or other applications to control the atomic motion, have motivated a series of theoretical studies to determine efficient atomic laser configurations and internal level structure, as well as to identify and quantify possible limitations.

In this paper we have investigated three-dimensional effects in an atom diode which had been ignored in the existing one-dimensional models. We have shown that the three-dimensional case can be reduced to one-dimensional Schrödinger equations with “effective” detunings taking into account Doppler and recoil effects. Simple formulae have been deduced for angle-dependent upper and lower velocity bounds for correct “diodic” behavior. The goal of a “diodic” behavior independent of the incident angle up to a maximum velocity, a requirement to implement, for example, the Maxwell pressure demon, can be realized by properly detuned lasers.

### Acknowledgments

We acknowledge “Acciones Integradas” of the German Academic Exchange Service (DAAD) and of Ministerio de Educación y Ciencia (MEC). This work has also been



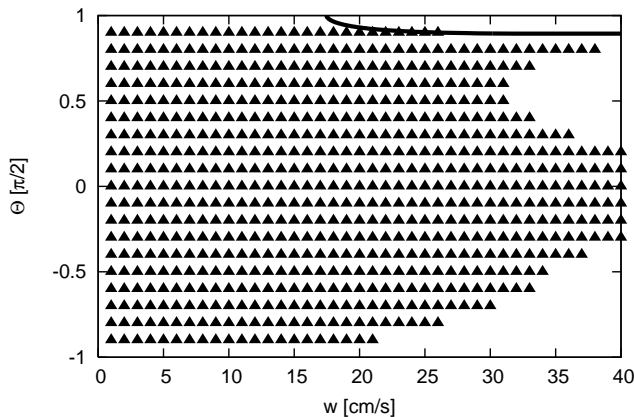


FIG. 8: Dioidic behavior based on 3 levels plus quenching: the filled triangles indicate full transmission to the third state without quenching laser and full absorption if a quenching potential is added;  $v_{Q0} = 3$  cm/s,  $\Delta v_Q = 0$ ,  $\widehat{\Omega}_Q = 2 \times 10^6$  s $^{-1}$ ,  $x_Q = 150$   $\mu$ m,  $\gamma_4 = 3 \times 10^5$  s $^{-1}$ , for other parameters see Fig. 7b.

supported by MEC through the project FIS2006-10268-C03-01, and by UPV-EHU (00039.310-15968/2004). AR acknowledges support by the Joint Optical Metrology Center (JOMC), Braunschweig.

#### APPENDIX A: EFFECTIVE STATE-SELECTIVE MIRROR POTENTIALS IN 3D

In this section we will generalize the results of [12] to the three-dimensional case. The objective is to justify the dependence assumed in the main text for the state-selective mirror potentials. We assume two levels connected with a detuned laser characterized by a wave vector  $k_L$  in  $y$  direction, a Rabi frequency  $\Omega(x)$ , and a large detuning  $\Delta$ . We shall also assume as before that the atom impinges on the laser region in the ground state with wave number  $k > 0$ . The wave vector  $\Psi = \begin{pmatrix} \psi_1 \\ \psi_2 \end{pmatrix}$  of the atom in the laser adapted interaction picture should obey the stationary Schrödinger equation,

$$H\Psi(x, y) = E\Psi(x, y)$$

where now

$$H = \frac{p^2}{2m} + \frac{\hbar}{2} \begin{pmatrix} 0 & \Omega(x)e^{-ik_L y} \\ \Omega(x)e^{ik_L y} & -2\Delta \end{pmatrix},$$

$E = \hbar^2 k^2 / 2m$ ,  $p^2 = p_x^2 + p_y^2$ ,  $\Omega(x)$  is the position dependent Rabi frequency,  $\Delta = \omega_L - \omega_{21}$  is the detuning between the laser frequency and the atomic transition frequency  $\omega_{21}$ . In components, we have:

$$E\psi_1(x, y) = \frac{p^2}{2m}\psi_1(x, y) + \frac{\hbar}{2}\Omega(x)e^{-ik_L y}\psi_2(x, y) \quad (\text{A1})$$

$$E\psi_2(x, y) = \frac{p^2}{2m}\psi_2(x, y) + \frac{\hbar}{2}\Omega(x)e^{ik_L y}\psi_1(x, y) - \hbar\Delta\psi_2(x, y). \quad (\text{A2})$$

We can write Eq. (A2) in the following way

$$\left[ E + \hbar\Delta - \frac{p^2}{2m} \right] \psi_2(x, y) = \frac{\hbar}{2}\Omega(x)e^{ik_L y}\psi_1(x, y),$$

and if  $\Delta$  is large it follows heuristically that

$$\psi_2(x, y) \approx \frac{\Omega(x)}{2\Delta}e^{ik_L y}\psi_1(x, y).$$

Putting this into equation (A1) we get

$$E\psi_1(x, y) \approx \frac{p^2}{2m}\psi_1(x, y) + \frac{\hbar}{2}W(x)\psi_1(x, y),$$

where

$$W(x) = \frac{\Omega(x)^2}{2\Delta},$$

i.e., there results a local and energy-independent approximation  $W(x)$  to the exact optical potential for state 1. Note that  $W(x)$  equals the one-dimensional effective potential derived in [12] and does only depend on  $x$  even in a three-dimensional case. It is also remarkable that it is energy and angle independent, and these properties rely on the possibility to neglect kinetic energies and Doppler terms with respect to the high detuning.

[1] D. E. Pritchard, A. D. Cronin, S. Gupta, D. A. Kokorowski, *Ann. Phys. (Leipzig)* **10**, 35 (2001).  
 [2] A. Ruschhaupt and J. G. Muga, *Phys. Rev. A* **70**, 061604(R) (2004).  
 [3] A. Ruschhaupt and J. G. Muga, *Phys. Rev. A* **73** (2006) 013608.  
 [4] A. Ruschhaupt, J. G. Muga, and M. G. Raizen, *J. Phys. B: At. Mol. Opt. Phys.* **39**, L133 (2006).  
 [5] M. G. Raizen, A. M. Dudarev, Qian Niu, and N. J. Fisch, *Phys. Rev. Lett.* **94**, 053003 (2005).

[6] A. M. Dudarev, M. Marder, Qian Niu, N. J. Fisch, and M. G. Raizen, *Europhysics Letters* **70**, 761 (2005).  
 [7] J. C. Maxwell, *Theory of Heat, 4th edition* (London: Longmans, Green and Co., 1875), p. 328-329.  
 [8] H. S. Leff and A. Rex (eds), *Maxwell's Demon: entropy, information, computing* (Princeton: Princeton University Press, 1990).  
 [9] H. S. Leff and A. Rex (eds), *Maxwell's Demon 2: entropy, classical and quantum information, computing* (Bristol and Philadelphia: Institute of Physics Publishing, 2003).

- [10] A. Ruschhaupt, J. G. Muga, and M. G. Raizen, *J. Phys. B* **39**, 3833 (2006).
- [11] K. Bergmann, H. Theuer, and B. W. Shore, *Rev. Mod. Phys.* **70**, 1003 (1998).
- [12] A. Ruschhaupt, J. A. Damborenea, B. Navarro, J. G. Muga, and G. C. Hegerfeldt, *Europhys. Lett.* **67**, 1 (2004).
- [13] G. C. Hegerfeldt and T. S. Wilser in: *Classical and Quantum Systems*. Proceedings of the Second International Wigner Symposium, July 1991, edited by H. D. Doebner, W. Scherer, and F. Schroeck, (Singapore: World Scientific, 1992), p. 104; G. C. Hegerfeldt, *Phys. Rev. A* **47** 449 (1993); G. C. Hegerfeldt and D. G. Sonderrmann, *Quantum Semiclass. Opt.* **8** 121 (1996). For a review cf. M. B. Plenio and P. L. Knight *Rev. Mod. Phys.* **70** 101 (1998). The quantum jump approach is essentially equivalent to the Monte-Carlo wave function approach of J. Dalibard, Y. Castin, and K. Mølmer *Phys. Rev. Lett.* **68** 580 (1992), and to the quantum trajectories of H. Carmichael, *An Open Systems Approach to Quantum Optics*, Lecture Notes in Physics m18 (Berlin: Springer, 1993).